

Being in Two Places at Once: Spin-Charge Separation

Mark Schubel

December 13, 2010

Abstract

High-energy experiments have shown that the electron is a point-like particle with spin-1/2 and electric charge $-e$. In highly correlated condensed matter systems these two properties can decouple in the lowest level excitations with the creation of two new quasiparticles: spinons (which carry spin) and chargons (which carry electric charge). I investigate the conditions under which this phenomena occurs, how common it is in nature and the experimental evidence for it, as well as look at the frontier in both theory and experiment in two-dimensional systems such as high-temperature superconductors and cold atom experiments.

Introduction

Quasiparticles naturally arise in nearly every condensed matter system due to interactions between the constituent “real” particles. While these particles are not real in that their existence is totally dependent on the many-body effects of the system and cannot be removed from the system, they can and do affect the physics and dynamics of the systems in which they arise. Also, like physical particles, quasiparticles have properties such as mass, spin, charge, momentum, etc. which are not required to match those of the underlying physical particles. One of the most unique examples of quasiparticle emergence is the case of spin-charge separation. Wherein a system (typically a gas of electrons) has two different quasiparticles: spinon, which carry spin and chargons which carry electric charge.

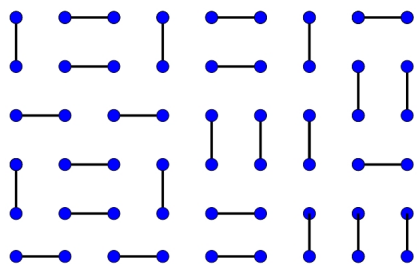


Figure 1: A schematic of a lattice of dimers. They are arranged so that the entire plane has charge $-Ne$ and zero spin [2]

This is perhaps best understood through a series of cartoons [2]. Consider a square lattice of electrons with one on each site. The electrons are paired in singlet states, and therefore have 0 spin (see figure 1). This system has electric charge $-Ne$ and spin 0. Suppose we unpair two of the electrons (figure 2), then the total system still has charge Ne , but has spin 1. By doing this we have created two spinons with spin-1/2. So despite the fact that in the underlying system charge and spin come together in an electron, we can create quasiparticles that while not carrying electric charge, can carry spin. Likewise, suppose we remove our unpaired electrons, and create two holes. Now the system again has 0 spin, but electric charge $-(N-2)e$, so we have created two holons (chargons with positive electric charge) with electric charge $+e$. In this paper I seek to answer a

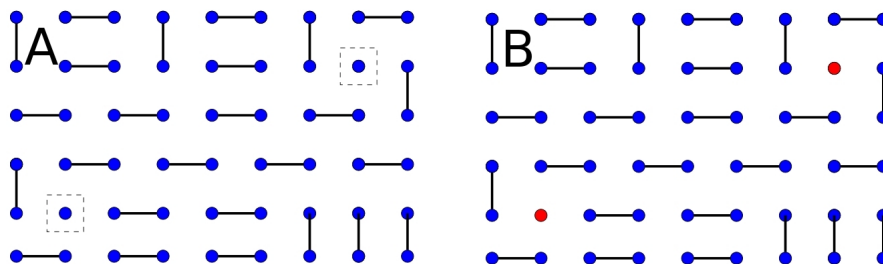


Figure 2: (A) Example of a system with two spinons, this is made by unpairing two of the electrons so that they are no longer in the spin-singlet state. Note that the system still has charge $-Ne$, so the excitations must not have any electric charge. (B) Example of system with two holons made by removing two electrons. The total system has zero spin, so the excitations have zero spin.[2]

few key questions about spin-charge separation. First, do actual real systems exist that exhibit this behavior? How universal is the emergence of spin-charge separation? And finally, what can studying the dynamics of spinons and holons tell us about novel condensed matter systems, such as high-temperature superconductors?

I will do this by demonstrating through bosonization that for one-dimesnional systems, spin-charge separation is a general phenomena, at least in the theory. With this

theoretical motivation, I continue by examining three systems of experimental interest: quantum nanowires, which are Tomonaga-Luttinger Liquids and also of great practical interest for applications in computing and nanotechnology, polyacetylene a long organic molecule of carbon and hydrogen atoms where the defects that divide the two degenerate ground states can create excitations that carry charge or spin but not both, and lastly we will look at SrCuO₂, where studies have shown that systems that are weakly correlated in two-dimensional systems become highly correlated in one-dimensional systems and therefore charge-spin separation emerges in these one-dimensional substances [4, 5, 7, 6].

These three experimental examples were also chosen because they use very different experimental techniques, yet all have confirmed spin-charge separation. The quantum wire experiment measured conductance and inter-wire tunneling to obtain a direct measurement of the spinon and chargin dispersion relations. The work with SrCuO₂ has recently obtained direct observations of two energy-momentum relations as well, but through a process known as angle-resolved photoemission, in which high energy photons knock electrons out of the substrate and measure their speed and direction to obtain information about the excitations in the substrate. In polyacetylene, the focus is on detecting the lowest-energy excitations and calculating the spin and charge of these excitations. This is done with nuclear magnetic resonance and measurements of electrical conductivity after chemical treatments, and has conclusively shown that both types of excitations exist independently.

I also discuss the experimental frontier, ultracold trapped atoms [9, 12]. These systems will provide cleaner and more controllable experiments than are currently available; however understanding the complex multi-body interactions and effectively trapping large numbers of fermions are both areas of current research. And finally we discuss the implications of this on high-temperature superconductivity, which is a problem that despite immense physical and practical interest has eluded scientists for years [10]. Theoretical models have predicted that this two-dimensional system may be one that has spin-charge separation, but more recent work has discounted some of the possible theories [1, 13].

Bosonization and Spin-Charge Separation

We will derive the key result of this paper in the low-energy limit (i.e. $|k| \sim k_F$) through a technique known as bosonization. Our results are in fact more general than they appear here, and are useful over a large energy range. However we will restrict ourselves to this limit for simplicity. Our work follows closely the derivation found in [3]. Bosonization is a technique in which a quartic Hamiltonian can be transformed into a quadratic one by pairing fermionic excitations into bosonic ones. It is a very general technique for studying highly correlated systems and is often the technique that is used to show that spin-charge separation does occur, even in higher-dimensional systems (however for simplicity we will limit ourselves to the one-dimensional case).

Our Hamiltonian is made of two parts, a kinetic energy component and interaction terms. Because we are only interested in the limit $k \sim k_F$, where k_F is the Fermi wavevector, our kinetic energy part is linear (this regime is that of the Tomonaga-Luttinger Liquid (TLL))

$$H_{kin} = \sum_{r=R,L} \sum_{\sigma=\uparrow,\downarrow} \sum_k v_F (\epsilon_r k - k_F) c_{r,k,\sigma}^\dagger c_{r,k,\sigma} \quad (1)$$

where R stands for right moving ($k \sim k_F$) and L stands for left moving ($k \sim -k_F$), ϵ_r takes the values $\epsilon_R = +1$ and $\epsilon_L = -1$, v_F is the Fermi velocity and c^\dagger and c are the fermionic creation and annihilation operators. We define the density fluctuation operator

by

$$\rho_{r,\sigma}(q) = \sum_k c_{r,k+q,\sigma}^\dagger c_{r,k,\sigma}$$

Now this operator is a bosonic operator since it is made of two fermionic ones. It is a logical choice for our Hamiltonian because it has a well-defined kinetic energy, namely $E_q = \pm v_F q$ for right and left moving particles respectively. Next we consider how this operator acts on the vacuum, most importantly

$$\rho_{L,\sigma}^\dagger(q > 0) |0\rangle = 0 \text{ and } \rho_{L,\sigma}^\dagger(q < 0) |0\rangle = 0$$

it suggests we should define the bosonic creation and annihilation operators from these operators as

$$b^\dagger(q, \sigma) = \sqrt{\frac{2\pi}{L|q|}} \sum_r \Theta(rq) \rho_{r,\sigma}^\dagger(q) \quad \text{and} \quad b(q, \sigma) = \sqrt{\frac{2\pi}{L|q|}} \sum_r \Theta(rq) \rho_{r,\sigma}(q) \quad (2)$$

where $\Theta(x)$ is the typical heavyside step function

$$\Theta(x) = \left\{ \begin{array}{ll} 1 & x > 0 \\ 0 & \text{otherwise} \end{array} \right\}$$

With our new definition, we can compute the commutation relations for $b(q, \sigma)$ and our Hamiltonian. We see

$$[b(q, \sigma), H] = v_f q b(q, \sigma)$$

and also obtain similar results for $b^\dagger(q, \sigma)$. If we assume completeness of the b 's, we can write our kinetic Hamiltonian in terms of only the b 's. The simplest way this can be done is

$$H = \sum_{p \neq 0, \sigma} v_F |p| b^\dagger(p, \sigma) b(p, \sigma) + \frac{\pi v_F}{L} \sum_r N_r \quad (3)$$

where N_r is the total number of left (or right) moving electron hole pairs. For the interaction part of the Hamiltonian it is more convenient to work in position space rather than momentum space. So we get

$$\psi_{r,\sigma}(x) = \sum_k e^{\epsilon_r k x} c_k^\dagger \quad (4)$$

$$\rho_{r,\sigma}(x) = \psi_{\sigma,r}^\dagger(x) \psi_{\sigma,r}(x) \quad (5)$$

We can likewise Fourier transform the bosonic operators (equation 2) and we find two bosonic fields $\phi_\sigma(x)$ and $\theta_\sigma(x)$ given by

$$\phi_\sigma(x) = -(N_R + N_L) \frac{\pi x}{L} - \frac{i\pi}{L} \sum_p \sqrt{\frac{L|p|}{2\pi}} \frac{1}{p} e^{-\alpha|p|/2 - ipx} (b^\dagger(p, \sigma) + b(-p, \sigma)) \quad (6)$$

$$\theta_\sigma(x) = (N_R - N_L) \frac{\pi x}{L} + \frac{i\pi}{L} \sum_p \sqrt{\frac{L|p|}{2\pi}} \frac{1}{p} e^{-\alpha|p|/2 - ipx} (b^\dagger(p, \sigma) + b(-p, \sigma)) \quad (7)$$

where α serves as a regulator. So one should consider the limit $\alpha \rightarrow 0$ only; however a finite α helps account for finite bandwidth which is present in experiment [3].

If we wish to find expressions for $\rho_{r,\sigma}(x)$ in terms of ϕ and θ , we need to note that

$$\begin{aligned} [\phi_\sigma(x), \nabla\theta_\sigma(y)] &= i \int_0^\infty dp \cos(p(x-y)) e^{-\alpha|p|} \\ &= i\pi\delta(x-y) \end{aligned}$$

which allows us to make the identification of the conjugate momentum to the field $\phi_\sigma(x)$

$$\Pi_\sigma(x) = \frac{1}{\pi} \nabla\theta_\sigma(x) \quad (8)$$

and likewise for the field $\theta_\sigma(x)$

$$\pi_\sigma(x) = \frac{1}{\pi} \nabla\phi_\sigma(x) \quad (9)$$

Using equations 6, 7, 8, and 9 we have

$$\rho_{r,\sigma}(x) = -\frac{1}{2\pi} [\nabla\phi_{r,\sigma}(x) + \epsilon_r \nabla\theta(x)] \quad (10)$$

For the interaction part of the Hamiltonian, we will only consider the lowest-three possi-

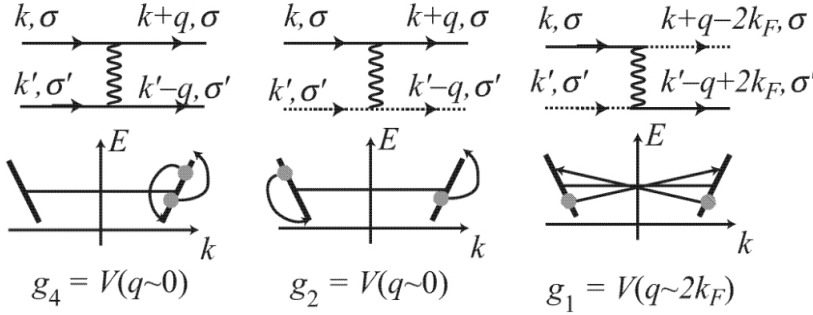


Figure 3: The dominant low-energy interactions are divided into three different types (labeled, for historical reason by g_i). In theories with spin (such as ours), each g_i can take two values $g_{i\parallel}$ and $g_{i\perp}$ depending if the spins are in the same direction ($g_{i\parallel}$) or in opposite direction ($g_{i\perp}$) [3]

ble terms, with momentum exchange, q , $q \sim 0$ and $q \sim 2k_F$ (see figure 3 for the diagrams of these interactions). These terms have the form

$$H_1 = \int dx g_{1\parallel} \sum_{\sigma} \psi_{L,\sigma}^\dagger \psi_{R,\sigma}^\dagger \psi_{L,\sigma} \psi_{R,\sigma} + g_{1\perp} \sum_{\sigma} \psi_{L,\sigma}^\dagger \psi_{R,-\sigma}^\dagger \psi_{L,-\sigma} \psi_{R,\sigma} \quad (11)$$

$$H_2 = \int dx g_{2\parallel} \sum_{\sigma} \psi_{R,\sigma}^\dagger \psi_{R,\sigma} \psi_{L,\sigma}^\dagger \psi_{L,\sigma} + g_{2\perp} \sum_{\sigma} \psi_{R,\sigma}^\dagger \psi_{R,-\sigma} \psi_{L,-\sigma}^\dagger \psi_{L,\sigma} \quad (12)$$

$$H_4 = \int dx g_{4\parallel} \sum_{\sigma,r} \psi_{r,\sigma}^\dagger \psi_{r,\sigma} \psi_{r,\sigma}^\dagger \psi_{r,\sigma} + g_{4\perp} \sum_{\sigma,r} \psi_{r,\sigma}^\dagger \psi_{r,-\sigma} \psi_{r,-\sigma}^\dagger \psi_{r,\sigma} \quad (13)$$

We wish to diagonalize this Hamiltonian. The first step is to define the total spin and total charge density

$$\rho(x) = \frac{1}{\sqrt{2}} [\rho_\uparrow(x) + \rho_\downarrow(x)]$$

$$\sigma(x) = \frac{1}{\sqrt{2}} [\rho_{\uparrow}(x) - \rho_{\downarrow}(x)]$$

With this definition, we get the following new boson fields

$$\phi_{\rho}(x) = \frac{1}{\sqrt{2}} [\phi_{\uparrow}(x) + \phi_{\downarrow}(x)]$$

$$\phi_{\sigma}(x) = \frac{1}{\sqrt{2}} [\phi_{\uparrow}(x) - \phi_{\downarrow}(x)]$$

Using our above definitions we find

$$H_{kin} = \frac{1}{2\pi} \int dx v_F [(\pi\Pi_{\sigma}(x))^2 + (\nabla\phi_{\sigma}(x))^2] + v_F [(\pi\Pi_{\rho}(x))^2 + (\nabla\phi_{\rho}(x))^2] \quad (14)$$

$$H_1 = \int dx (-g_{1\parallel} \sum_{\sigma} [\rho_{L,\sigma}, \rho_{R,\sigma}] + \frac{g_{1\perp}}{2(\pi\alpha)^2} \cos(2\sqrt{2}\phi_{\sigma}(x))) \quad (15)$$

$$H_2 = \frac{1}{4\pi^2} \int dx [g_{2\parallel} + g_{2\perp}] [(\nabla\phi_{\rho}(x))^2 - (\nabla\theta_{\rho}(x))^2] + [g_{2\parallel} - g_{2\perp}] [(\nabla\phi_{\sigma}(x))^2 - (\nabla\theta_{\sigma}(x))^2] \quad (16)$$

$$H_4 = \frac{1}{4\pi^2} \int dx [g_{4\parallel} + g_{4\perp}] [(\nabla\phi_{\rho}(x))^2 + (\nabla\theta_{\rho}(x))^2] + [g_{4\parallel} - g_{4\perp}] [(\nabla\phi_{\sigma}(x))^2 + (\nabla\theta_{\sigma}(x))^2] \quad (18)$$

So we see that our Hamiltonian breaks into two parts: a charge-density part and a spin-wave part, so we can write

$$H = H_{\rho} + H_{\sigma} \quad (19)$$

Since these two parts of the Hamiltonian are independent and do not interact, that means these theories span a Hilbert space made of two separate spaces: one for spin-waves and the other one for charge-density waves. These two excitations are therefore totally separate and will move independently of one another [3].

Our above derivation is very general in the low-energy limit. We did not make any assumptions about the substance other than 1) there exists as a well-defined Fermi wavevector and velocity (which is generally true for fermionic systems by the Pauli Exclusion Principle) and that 2) we are only interested in excitations near that Fermi-level.

Polyacetylene

Polyacetylene is a long hydrocarbon lattice. In the ground-state, the lattice breaks into two sub-lattices, we will call them A and B, with the carbon atom offset from the standard lattice point by a small amount either to the right (for lattice A) or left (lattice B). This splitting causes there to be two degenerate ground states, depending on which lattice moves right or left (see figure 4). The lowest-level excitations, called solitons, are

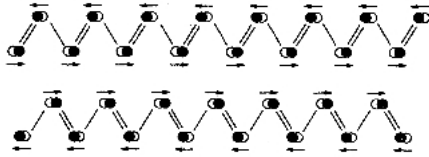


Figure 4: A schematic diagram of the two degenerate ground states of polyacetylene, note how the carbon atoms are moved slightly from their expected ground-state positions [4]

topological in nature and represent bond changes when going from one of the degenerate ground states to the other. This permits three possible lowest-energy states: two charged soliton states with charge +e or -e (holon or chargin respectively) and no spin, and an uncharged soliton state with spin-1/2 (figure 5). Since there are two main types of solitons charged solitons (chargin and holons) and uncharged (spinon), experiments have taken

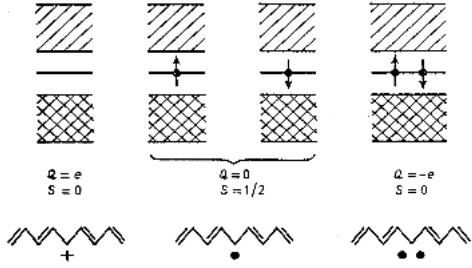


Figure 5: The three lowest energy excitations for polyacetylene. (left) A holon with no spin and electric charge $+e$. (center) A spinon with no electric charge and spin-1/2. (right) A chargon with no spin and electric charge $-e$. [4]

different techniques to find these two states. Neutral solitons are studied using nuclear magnetic resonance [4]. These studies have demonstrated that these solitons do exist, and are uncharged. While, the existence was easy to demonstrate, showing that these are indeed without charge was more difficult. The key experiment was to compensate for the electrical conductivity with ammonia. While the number of charge carriers and electrical conductivity both decreased dramatically, the number of spins did not change [4]. Charged solitons are primarily investigated through one of three signatures [4]. The first is through the formation of localized phonons. These states have a characteristic vibrational mode that is dominant in the infrared. The next is through the generation of a midgap state and the electronic transitions that induces. This again is observed in the near-infrared. The last is through charge storage in spinless solitons, which can be proved with electron-spin resonance experiments. This has been done and the ratio of the number of spins to number of charges has been found to be quite small $N_s/N_q \ll 1$). So both types of solitons have been extensively studied and demonstrated through both direct and indirect means as existing.

Quantum Wires

Much of the experimental interest in spin-charge separation is in its implications for nanowires and computation, so there is a relatively large amount of experimental work done on these systems. These systems are some of the simplest manifestations of the Tomonaga-Luttinger Liquids as often the underlying lattice is unimportant and the motion of the electrons can be considered as a one-dimensional sea of electrons. The experiment consisted of many $17.5\mu\text{m}$ long nanowires of lithographic width $.17\mu\text{m}$ (see figure 6). The ends of the wires were attached to gates that could control voltage. The conductance through the wires was then measured using a two dimensional Fermi-gas. This was chosen to allow the probe to obey different physics than the experimental apparatus. A tunable magnetic field was placed across the wires to change the spectral overlap between the wires and see how that influenced tunneling between the wires. The different dispersion relations for holons and spinons should manifest themselves in measurements of the conductance, G , at different gate voltages and magnetic field values. To better emphasize the changes in G with magnetic field, often dG/dB is plotted instead (this also follows the dispersion relations).

Figure 6 compares dG/dB in theory and experiment. The experimental data clearly has a feature (denoted by a red line) that does not match the theoretical predictions of the non-interacting theory. This feature is identified as the chargon distribution, and is predicted by the TLL theory (figure 6E).

There are two key features of the dispersion relations shown in figure 7. The first is that of the one-dimensional parabola. This comes from the spin excitations since these have a velocity that is roughly the same as the Fermi velocity. The second is a step linear

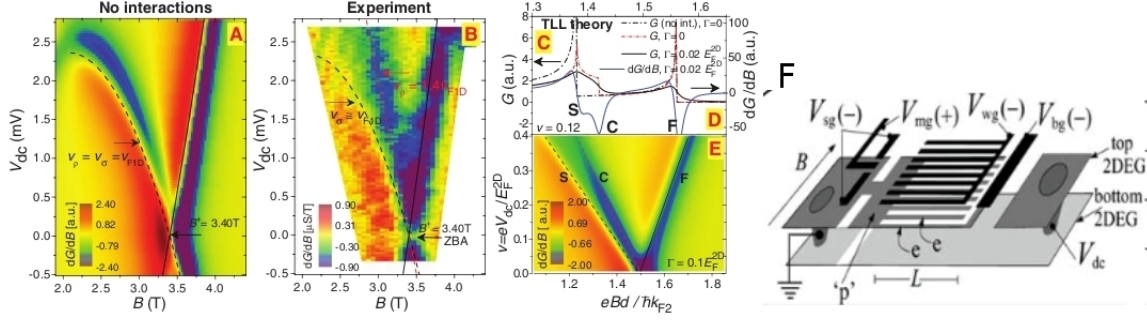


Figure 6: A comparison of dG/dB for theory and experiment. (A) The noninteracting plot. The singularities follow the non-interacting parabola, which is as expected. (B) Experimental results. The experimental data clearly does not follow the non-interacting parabola, which is to be expected. (C) Calculation of G and (D) dG/dB for the non-interacting and TLL models. (E) The predictions of TLL theory. This has the same features as the experimental result, we identify S as the spinons and C as the chargons. (F) Schematic of wire-tunneling experiment to measure spin-charge separation. The signs on the gates denote voltage sign. [5]

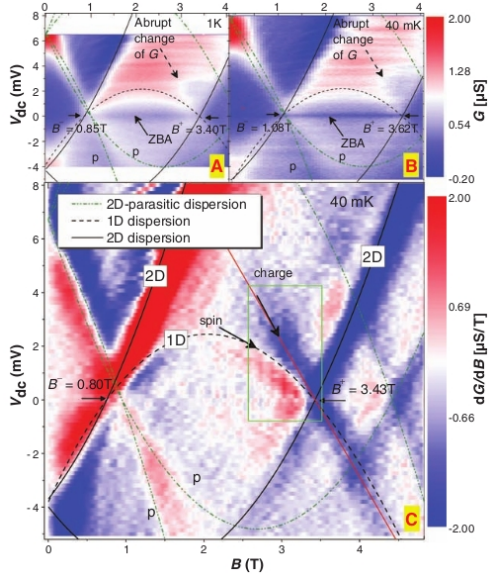


Figure 7: (A and B) Color-scale plots of G versus V and B at two different temperatures. The black dotted line represents expected singularities in G , as predicted from the noninteracting theory, while the green lines are from 2D-2D tunneling. There are two features that are not predicted in the non-interacting theory, the first is the marked abrupt change in G , and the other is the zero bias (labeled ZBA). (C) dG/dB . The straight red line is clearly not part of the 1 or 2 D dispersion, and is identified with the chargon, while the 1-D dispersion relation is from the spinon. [5]

relation that is caused by the chargons. We would expect this since the chargons have a much higher velocity, and can therefore identify the sources of both dispersion relations. The plots of G (figures 7 A and B) show that two features that cannot be explained by a non-interacting theory. The first is that at zero bias, G is highly suppressed, while the second is an abrupt change in G .

Also, this experiment was able to observe spin-charge separation well past the low-energy limit (and hence beyond the linear-kinetic energy regime in which the TLL model should be valid). Renormalization-group calculations have suggested this, as higher order perturbations only lead to renormalizing the TLL parameters.

SrCuO₂

In one-dimensional systems all excitations are highly correlated since atoms cannot move without encountering other particles. This leads to the break down of Fermi-liquid theory in one-dimension, so if a system does not exhibit spin-charge separation in two-dimensions, it is reasonable to assume it will in one-dimension. This has been tested experimentally using a one-dimensional and two-dimensional strontium compounds [7].

The experiment used angle-resolved photoemission to measure the energy versus momentum relationship for SrCuO₂, which due to weak inter-chain coupling between is nearly a one-dimensional system, and compared that two literature measurement made for the two-dimensional. Sr₂CuCl₂O₂.

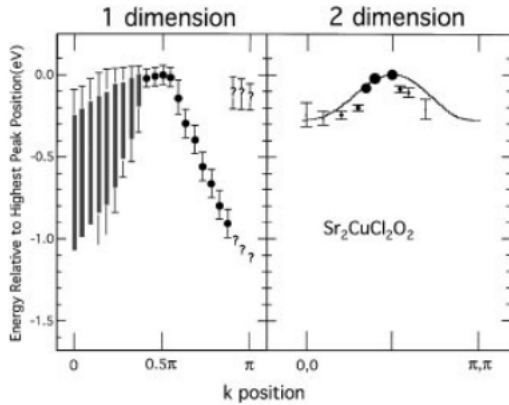


Figure 8: E vs k relationship for the one and two-dimensional case. Note that in the one-dimensional case there are two bands in the range $\pi/2 < k < \pi$, while there is only one for the two dimensional case. [7]

One of the most striking results of this experiment was the difference in energy versus wavevector for the one-dimensional SrCuO₂ versus the (previously observed) data for the two-dimensional Sr₂CuCl₂O₂ (see figure 8). In the regime $k \sim \pi$ two bands appear, which is indicative of spin-charge separation, however there is some uncertainty about the values of these points due to their weak signal [7].

Another experiment using SrCuO₂ studied the the spinon and holon dispersions also using angle-resolved photoemission [6]. In angle-resolved photoemission, electrons are knocked out of the substance, and the angle and speed of the removed is measured. For typical substances where spin-hole separation does not occur, the resulting holon should simply move around and a single excitation spectrum exists. However, in spin-charge separation occurs, the created holon will decay into a spinon and holon (without spin), and causes the creation of two branches with edge singularities.

While the technique of angle-resolved photoemission should be able to resolve two different peaks and provide direct evidence for spin-charge separation, direct observation was quite difficult until recently. Unlike previous groups, Kim et al. used high-energy photons that had previously not been possible, which allowed them to excite electrons beyond the high-energy oxygen states that exist in SrCuO₂ [6]. The result was two peaks in the energy distribution curves for k_{\parallel} , the momentum parallel to the plane of the substance. The quickly fading peak was associated with the holon, while the slowly decaying peak with the spinon (figure 9). In the raw data the two peaks are clearly visible (figure 9) which are due to the dispersion of chargons and holons. The relative widths are plotted using a shown background that rises with energy [6].

There are two main features that cannot be described by the theory. The first is the part of the spectrum that is shown in green figure 9A. Another aspect of the found function that cannot be explained by the theory is why it is so broad. The theory expects sharp edges, and since the experimental resolution is much smaller than the

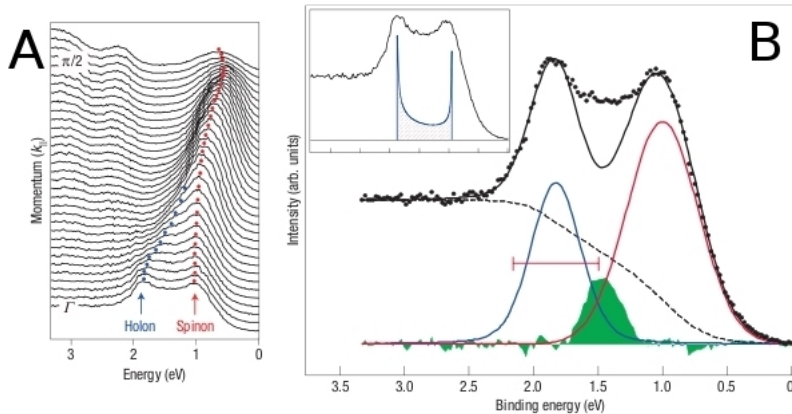


Figure 9: (A) Energy-momentum relation. The two peaks are identified with spinons (shown in red) and holons (shown in blue). (B) Raw data (black dots) with fitted spinon (blue line) and chargon (red line) Gaussian curves. The background was accounted for by the rising dotted line. The green shaded region is unaccounted for spectrum [6].

effect. Possible explanations include next-nearest-neighbor hopping, interactions with other orbitals, temperatures or lattice effects [6]

Ultracold Quantum Gases

Ultracold atomic gases provide a new windowing into condensed matter systems by providing a highly controlled and clean experimental apparatus with which to compare theory to experiment. This makes them an ideal for studying highly-correlated systems. While bosonic systems are extensively studied, fermionic systems are significantly more difficult both in theory and in practice. However, more experiments are being proposed that would use cold fermionic systems to study highly correlated systems [12], and numerical studies are ongoing to examine what the results should look like from these systems [9]. However, what is measured in systems of atomic gases is not truly spin-charge separation, but instead the separation of density waves and hyperfine energy levels. Though we will still refer to this as spin-charge separation (as is common in the literature) and make the identification chargon \rightarrow density wave and spinon \rightarrow hyperfine splitting between two energy states.

Recati et al. [12] suggested trapping cold atoms in a harmonic potential, then by shining a short-laser pulse near the center of the gas, a spin or charge wavepacket could be excited. With additional laser pulses, the movement of the packets could be measured and analyzed. Since the two types of packets will move at different velocities, this would provide direct evidence of spin-charge separation [12].

Numerical studies are also ongoing. The computational work to study fermionic systems with spin is much greater than typical bosonic systems, however Kollath et al were able to compute the movement of a spin and charge wave in a system similar to that proposed by Recati et al [9].

Their work found spin-charge separation by creating a spin and charge wave at the same point at a time, and measuring how these packets evolved in time. They found that the created wave splits into four component waves, two spin waves and two charge waves. Both waves of each time have the same speed, but move in opposite directions, while the charge and spin waves have distinct speeds [9].

In short, while ultracold atoms have not been extensively studied for spin-charge separation yet, they will surely be an important experimental environment in the future. The ability to have complete control over the system and extremely clean samples means

that experiment and theory could be tested like never before.

Applications to High-Temperature Superconductivity

The cuprate superconductors are a class of superconductors made of a copper mixture (generally Copper-Oxide layers with nearby layers of other ions such as Barium, Lanthanum, or Strontium) which have been observed to superconduct in temperatures as high as $\sim 100K$ [10]. However, no mechanism has yet been demonstrated that can explain why these materials are superconductors over this range of temperatures.

There are a few qualitative reasons to believe that spin-charge separation may play a role in high-temperature superconductors, especially the cuprates. The first is the quasi-two dimensional nature of these substances [10]. No example of spin-charge separation has yet been proposed in dimensions greater than two, though there is increasing evidence that two-dimensional systems do exhibit this phenomena [8][11]. Furthermore, the electrons in these systems are believed to be highly-correlated, which is the common feature of all of the systems in which spin-charge separation has been found.

Besides the wide range over which the cuprates are superconductors, another intriguing property of these materials is that, in their normal phases (i.e. when they are not superconductors) over a wide range of temperatures, resistivity and temperature are proportional. This is strange because typically the cuprates are treated as quasi-two dimensional systems, so in the normal phase this suggests that they would follow Fermi-liquid theory in the normal phase. However, in Fermi-liquid theory, the resistivity of a material is dominated by electron-phonon interactions, which leads to a quadratic dependence on temperature, not linear. This suggests that even the normal state is not a canonical Fermi-liquid.

Spin-charge separation can cause a linear temperature-electrical resistivity relation and because of this is a reasonable point to consider what effects this phenomena can have on superconductors. Si [13] found that by assuming spin-charge separation, one finds that the spin and charge electrical resistivities are different, in fact while the electrical resistivity is linear, as expected the spin resistivity went as $T^{4/3}$. This is in contrast to the theory where spin and charge cannot separate, in which both of the resistivities must be the same (and scale quadratically for $T \ll T_c$ and linearly for $T \gg T_c$)

However, there are limits on how strong this effect can be. Due to an absence of observed vortex states (known as vortices) in the cuprate superconductors, it was shown that the at least one class of spin-charge separation models cannot be valid for the cuprates [1].

Until direct experimental evidence, or a complete model for superconducting is found for the cuprates and other high-temperature superconductors, it is unlikely this debate will be fully resolved. Unfortunately, as we have seen in the one-dimensional cases above, observing spin-charge separation directly is often quite difficult and challenging, and there are no known methods that have observed spin-charge separation in any two-dimensional system. However some methods have been proposed to test Si's work, including measurement of the change in magnetization of one end of a superconducting sample as spin-polarized current is injected into it [13].

Discussion

While the theory of spin-charge separation is well-developed for one-dimensional systems, the experimental results have, until recently been lacking. However, recent technologi-

cal developments have allowed for the direct measurement of distinct holon and spinon dispersion relations in quantum wires and SrCuO₂. Meanwhile measurement of charged, spinless and uncharged spin-1/2 solitons in polyacetylene has further shown that these two types of excitations exist independently of one other.

So while the existence of spin-charge separation is both predicted and observed in one-dimension, the next experimental breakthroughs are likely to occur in cold atom experiments where the ability to precision control the parameters of the experiment will allow for unparalleled measurements of degree of freedom splitting.

From a theoretical perspective, the frontier lies in higher-dimensional systems such as quantum spin hall states, RVB states in ferromagnets and high-temperature superconductors. While these two-dimensional models can allow for spin-charge separation, the theories are far from certain. Once experimentally verifiable predictions become available, this will provide another frontier to test the theory of spin-charge separation.

Despite the questions this phenomena could answer about highly correlated physics, it opens a potential Pandora's Box for new physics. Can other properties that are considered intrinsic to particles separate in condensed matter systems? What are the implications of these excitations on what we consider "fundamental"?

References

- [1] D. A. Bonn, Janice C. Wynn, Brian W. Gardner, Yu-Ju Lin, Ruixing Liang, W. N. Hardy, J. R. Kirtley, and K. A. Moler, *A limit on spincharge separation in high- T_c superconductors from the absence of a vortex-memory effect*, Nature **414** (2001), 887–889.
- [2] Paul Fendley, *Fractional charge colloquium*, Slides available at: <http://rockpile.phys.virginia.edu/>.
- [3] Thierry Giamarchi, *Quantum physics in one dimension*, Oxford University Press, 2003.
- [4] A. J. Heeger, S. Kivelson, J.R. Schrieffer, and W.P Su, *Solitons in conducting polymers*, Rev Mod Phys **60** (1988), 781–850.
- [5] Y. Jompol, C. J. B. Ford, J. P. Griffiths, I. Farrer, G. A. C. Jones, D. D. A. Ritchie, T. W. Silk, and A. J. Schofield, *Probing spin-charge separation in a tomonaga-luttinger liquid*, Science **325** (2005), 597–601.
- [6] B. J. Kim, H. Koh, E. Rotenberg, S.-J. Oh, H. Eisaki, N. Motoyama, S. Uchida, T. Tohyama, S. Maekawa, Z.-X. Shen, and C. Kim, *Distinct spinon and holon dispersions in photoemission spectral functions from one-dimensional SrCuO₂*, Nature **2** (2006), 397–401.
- [7] C. Kim, A. Y. Matsuura, Z.-X. Shen, N. Motoyama, H. Eisaki, S. Uchida, T. Tohyama, and S. Maekawa, *Observation of spin-charge separation in one-dimensional SrCuO₂*, Phys Rev Lett **77** (1996), 4054–4057.
- [8] S. A. Kivelson, *Electron fractionalization*, Synthetic Metals **125** (2002), 99–106.
- [9] C. Kollath, U. Schollwöck, and W. Zwerger, *Spin-charge separation in cold fermi gases: A real time analysis*, Phys Rev Lett **95** (2005), no. 176401.
- [10] Anthony J. Leggett, *What do we know about high T_c ?*, Nature **21** (2006), 134–136.
- [11] Xiao-Liang Qi and Shou-Cheng Zhang, *Spin charge separation in the quantum spin hall state*, Phys Rev Lett **101** (2008), no. 086802.
- [12] A. Recati, P. O. Fedichev, W. Zwerger, and P. Zoller, *Spin-charge separation in ultracold quantum gases*, Phys Rev Lett **90** (2003), no. 020401.
- [13] Qimiao Si, *Spin conductivity and spin-charge separation in the high- T_c cuprates*, Phys Rev Lett **78** (1997), 1767–1770.